ACS APPLIED MATERIALS & INTERFACES

Article

Copolymer Brushes with Temperature-triggered, Reversibly Switchable Bactericidal and Antifouling Properties for Biomaterial Surfaces

Bailiang Wang, Qingwen Xu, Zi Ye, Huihua Liu, Quankui Lin, Kaihui Nan, Yunzhen Li, Yi Wang, Lei Qi, and Hao Chen

ACS Appl. Mater. Interfaces, **Just Accepted Manuscript** • DOI: 10.1021/acsami.6b08893 • Publication Date (Web): 23 Sep 2016

ACS Publications

ACS Applied Materials & Interfaces is published by the American Chemical Society. 1155 Sixteenth Street N.W., Washington, DC 20036

Copolymer Brushes with Temperature-triggered, Reversibly Switchable Bactericidal and Antifouling Properties for Biomaterial Surfaces

Bailiang Wang[a, b] *, Qingwen Xu[a], Zi Ye[a], Huihua Liu[b], Quankui Lin[a, b], Kaihui Nan[a, b],Yunzhen Li[b], Yi Wang[b], Lei Qi[a] and Hao Chen[a, b] *

[a]School of Ophthalmology & Optometry, Eye Hospital, Wenzhou Medical University, Wenzhou 325027, China
[b]Wenzhou Institute of Biomaterials and Engineering, Chinese Academy of Sciences, Wenzhou 32500, China

*Corresponding authors
Fax: +86 577 88067962
E-mail: wangbailiang2006@aliyun.com (B. L. Wang); Chenhao823@mail.eye.ac.cn (H. Chen)

ABSTRACT
The adherence of bacteria and the formation of biofilm on implants is a serious problem that often leads to implant failure. A series of antimicrobial coatings have been constructed to resist bacterial adherence or to kill bacteria through contact with or release of antibacterial agents. The accumulation of dead bacteria facilitates further bacterial contamination and biofilm development. Herein, we have designed and constructed a novel, reversibly switchable bactericidal and antifouling surface through surface-initiated reversible addition-fragmentation chain transfer (RAFT) polymerization to combine thermally responsive N-isopropylacrylamide (NIPAAm) and bactericidal quaternary ammonium salts (2-(dimethylamino)-ethyl methacrylate ($DMAEMA^+$)). Measurements of spectroscopic ellipsometry, water contact angle and X-ray photoelectron spectroscopy were used to examine the process of the surface functionalization. The temperature-responsive P($DMAEMA^+$-*co*-NIPAAm) copolymer coating can switch by phase transition between a hydrophobic capturing surface at high temperature and a relatively hydrophilic antifouling surface at lower temperature. The quaternary ammonium salts of $PDMAEMA^+$ displayed bactericidal efficiency against both *Escherichia coli* and *Staphylococcus aureus*. The functionalized surface could efficiently prevent bovine serum albumin adsorption and had good biocompatibility against human lens epithelial cells.

Keywords: PNIPAAm; switchable antimicrobial; quaternary ammonium salts; antifouling; implant

1. INTRODUCTION

Biofouling such as nonspecific protein adsorption, bacterial adherence, and subsequent biofilm development is a ubiquitous problem(*1-3*). Although great efforts have been paid to the designing and constructing of antimicrobial surfaces, only in Europe, implants-related infections account for

approximately 50% of nosocomial infections, which greatly increased the economic burden and patient suffering(*4-6*). There are two main categories of antibacterial surfaces: (1) bacterial anti-adhesion surfaces(*7-9*) such as hydrophilic coatings based on poly(ethylene glycol) (PEG), poly(vinylpyrrolidone) (PVP), and zwitterionic polymers, etc.; and (2) bactericidal surfaces that function through contact killing using components such as quaternary ammonium salts, chitosan, etc., or antibacterial agent-loaded surfaces that release antibiotics or silver ions, etc.(*7, 10-12*). However, bacterial anti-adhesion surfaces are irreversibly contaminated by many kinds of proteins such as fibronectin, fibrin, and fibrinogen, and by platelets, which promote bacterial adhesion by providing donors(*13, 14*). Dead bacteria can easily accumulate on surfaces, which promotes further bacterial contamination and the formation of biofilms(*15-17*). Consequently, the ideal antibacterial surface should be capable of reversibly switching between broad-spectrum bactericidal activity and the release of dead bacteria by combining stimuli-responsive components(*18-20*). Jiang *et al.* have developed various kinds of smart antibacterial surfaces based on zwitterionic polymers that are able to simultaneously kill and release bacteria(*21-24*). For instance, Jiang and Cao developed a smart polymer that can be induced to switch repeatedly between killing attached bacteria and releasing dead bacteria simply by changing the pH of the aqueous environment(*21*). Yu and Chen have also constructed many kinds of smart antibacterial coatings that are able to capture and release bacteria in a controlled manner(*3, 25, 26*).

These smart antibacterial surfaces are mainly sensitive to environmental factors such as thermal-responsive, pH-responsive, enzyme-responsive and photo-responsive and so on(*4, 27-29*). As a typical thermol-responsive polymer, the lower critical solution temperature (LCST) of poly(N-isopropylacrylamide) (PNIPAAm) is about 32°C(*25, 30, 31*). PNIPAAm-based polymer surfaces are able to switch from being relatively hydrophobic at higher temperatures, which facilitates bacterial adherence, to being relatively hydrophilic at lower temperatures, which causes the release of bacteria(*32, 33*). Furthermore, the degree of temperature response of a PNIPAAm-based surface could be adjusted by changing the chain length, the grafting density, and the proportion of PNIPAAm and other antibacterial polymers(*34, 35*). Yu *et al.* have developed oligo(p-phenylene-ethynylene)/PNIPAAm films that showed efficient photo-responsive bactericidal property and on-demand bacteria-releasing functionality(*36*). Our group has constructed a water-erodible $(\text{heparin/chitosan})_{10}$−$(\text{poly(vinylpyrrolidone)/poly(acrylic acid)})_{10}$ ($(\text{HEP/CHI})_{10}$−$(\text{PVP/PAA})_{10}$) layer-by-layer (LBL) self-assembly film that is top-down degradable over a determined period of time and almost completely eliminates bacterial adhesion within 24 h(*13*). Furthermore, after total degradation of the hydrogen-bonded $(\text{PVP/PAA})_{10}$ LBL films, the bottom $(\text{HEP/CHI})_{10}$ LBL film still facilitated bactericidal contact killing(*37*). However, such antibacterial surfaces lack self-cleaning and reversibly switchable antimicrobial functionality.

Surface-initiated polymerization of polymer brushes is an important approach to achieving surface modification; the polymerization can be implemented using either “grafting onto” or “grafting from” methods(*38*). The “grafting from” method has two main advantages: (1) the surface features can be predictably tuned by changing the component of the brushes; and (2) the polymers have strong long-term stability because of the high chemical and mechanical robustness. What’s more, the “grafting from” method utilizing initiators on the surface to initiate polymerization and high grafting density brushes can be obtained(*8, 39*). Comparing with other controlled radical polymerizations, reversible addition-fragmentation chain-transfer (RAFT) polymerization is well known for its compatibility with a wide range of monomers(*40, 41*). In

addition, antibacterial agents such as chitosan, phosphonium salts, quaternary ammonium salts and antimicrobial peptides can be prepared on biomaterial surfaces and can exert very efficient bactericidal function through contact killing(*5, 7, 11, 15*). However, general polycation bactericidal surfaces release very few dead bacteria to restore and maintain long-acting efficient bactericidal function. Positively charged polycations adhere tightly to bacteria with negative charges. The existence of bacterial corpses promotes bacterial adhesion, which exacerbates the problem(*42, 43*). Therefore, a smart antibacterial surface that possesses both reversibly switchable and efficient bactericidal function and the ability to release dead bacteria is urgently required.

In the present work, copolymer brushes of poly(2-(dimethylamino)-ethyl methacrylate-*co*-NIPAAm)) (P(DMAEMA$^+$-*co*-NIPAAm)) were synthesized through RAFT polymerization to endow the substrates with reversibly switchable bactericidal and fouling release functionalities. The surface modification process was monitored by X-ray photoelectron spectroscopy (XPS), spectroscopic ellipsometry, atomic force microscopy (AFM) and water contact angle (WCA) measurements. The switch between the two surface states of capturing/killing and fouling/releasing induced by lowering the temperature from 37 to 4°C was detected by live/dead staining and shake-flask culture methods against *Staphylococcus aureus* (*S. aureus*) and *Escherichia coli* (*E. coli*). Fluorescein diacetate (FDA) and cell counting kit-8 assays (CCK-8) tests were used to determine cell compatibility of the brush coating with respect to human lens epithelial cells (HLECs). Such P(DMAEMA$^+$-*co*-NIPAAm) polymer brushes with temperature-triggered, reversibly switchable bactericidal and antifouling properties may be useful as surface modifiers for biomaterials.

2. MATERIALS AND METHODS

2.1. Reagents and materials

Polydimethylsiloxane (PDMS) (Sylgard® 184) from Dow Corning was used to prepare in accordance with the instructions. 4,4′-azobis-(4-cyanovaleric acid) (V501), 4-Cyano-4-(phenylcarbonothioylthio) pentanoic acid (RAFT agent), NIPAAm, DMAEMA, polyethyleneimine (PEI), 1-bromoheptane, 5-ethynyl-2′-deoxycytidine (EDC), and N-hydroxysulfosuccinimide (NHSS) were bought from Sigma-Aldrich. We used ultrapure distilled water from the Milli-Q Millipore system (Merck, USA).

2.2. Pretreatment of the substrates

Glass, PDMS, and silicon wafer substrates were cut into small pieces (1×2 cm^2) before cleaning with ethanol and subsequently with water. After being dried in N_2, the substrates were then aminated for 4 h with PEI solution (5 mg/mL) at room temperature.

2.3. Synthesis of P(DMAEMA$^+$-*co*-NIPAAm) copolymer brush coating

DMAEMA$^+$ monomers in ethanol (0–10 mg/mL) were first prepared by blending DMAEMA and 1-bromoheptane overnight in a molar ratio of 1:1. According to the literature, C6-C8 alkyl chain length endowed the quaternary ammonium salts with a much higher bactericidal property(*44, 45*). Therefore, 1-bromoheptane was used for quaternization in this work. Water was used to dilute the obtained mixing solution to a determined volume and titrated using 0.01 M NaOH with phenolphthalein as indicator. Degree of quaternization of DMAEMA$^+$ was calculated as ~89%. To immobilize RAFT agent, the aminolysed substrate was placed in the mixture of NHSS (20 mmol),

EDC (10 mmol) and RAFT agent (0.0234 mmol) in 2-(N-morpholino) ethanesulfonic acid (MES) buffer (0.1 M, pH 5.5) for 12 h with magnetically stirring. Then the P(DMAEMA$^+$-*co*-NIPAAm) copolymer brush coatings were synthesized through grafting of DMAEMA$^+$/NIPAAm monomer in ethanol at mass ratios of 0:10, 3:7, 5:5, 7:3, and 10:0, and the obtained samples were named P0-10, P3-7, P5-5, P7-3, and P10-0, respectively. And P′3-7 was representative of the P(DMAEMA-*co*-NIPAAm) copolymer brushes without quaternization of the DMAEMA monomers.

The typical synthesis process of P(DMAEMA$^+$-*co*-NIPAAm) (in the mass ratio of 3:7) is described as follows***(46)***. V501 (2 mg) and NIPAAm (35 mg) were fed into the 3-mL DMAEMA$^+$ (15 mg) ethanol solution in a 5-mL bottle under a nitrogen atmosphere. The substrates grafted with the RAFT agents were placed in the blended solution. Under magnetically stirring, the mixture was purged with nitrogen to discharge oxygen and then temperature was raised to 60°C to start the synthesis of the brushes. The polymerization was then carried out at the elevated temperature. After 24 h, the substrate was washed by ethanol for 10 min and dried in N_2.

2.4. Characterizations of the surface

2.4.1. Wettability and morphology

The wettability of the surfaces was measured using a DSA10 Mk2 Drop Shape analyzer (Krűss). All of the samples were placed in the incubator for 30 min with the temperature set at 4°C or 37°C and the testing process was done quickly to minimize the temperature changing. After fixing the sample, an ultrapure water droplet was dropped out to contact with the sample for 15 s. Image was taken by built-in microscope and the software was used to calculate the water contact angle (WCA) of the copolymer brush coating. AFM (SPA 400, Seiko Instruments, Inc.) was used to investigate the surface morphology of the coatings in the tapping mode in air using a commercial scanning probe microscope.

2.4.2. Coating thickness

Spectroscopic ellipsometry (M-2000 DITM, J.A. Woollam) was used to measure the thickness changes during the process of PEI amination, RAFT agent immobilization and copolymer brushes synthesis. To increase the intensity of reflected light, silicon wafer was used as substrate instead of PDMS sheet in this measurement. A continuous wavelength of 124–1700 nm and incidence angles of both 70° and 65° were used in the measurement. The Cauchy model was performed to automatically calculate the thickness that most closely fitted the copolymer brushes.

2.4.3. X-ray photoelectron spectroscopy (XPS)

A PHI 5300 ESCA System (PerkinElmer Co., USA) was used to collect the XPS spectra of the surfaces and the excitation wavelength of Al Kα was 1486.6 eV. The 45° take-off angle was used in the test and the X-ray source power was 250 W (12.5 kV). The survey was conducted to collect high resolution spectra with the binding energy range set at 0–1000 eV.

2.4.4. Gel permeation chromatography (GPC)

RAFT agent was fed into the DMAEMA$^+$/NIPAAm monomer solution to measure the molecular weight. The measurement was conducted on a Waters GPC system equipped with a set of Waters Styragel columns, a Waters-2487 dual λ absorbance detector, and a Waters-2414 refractive index

detector. HPLC grade THF was used as the diluent at a low flow rate of 1.0 mL/min. A series of near-monodisperse polystyrene standards were used in the calibration.

2.5. Cytotoxicity tests

2.5.1. Cell cultivation

The HLECs (from ATCC, SRA01/04) were incubated in Dulbecco's modified Eagle's medium (DMEM)/F12 (1:1) mixture supplemented with streptomycin (100 μg/mL), fetal bovine serum(10 wt%) and penicillin (100 U/mL) in a 5% CO_2 incubator at 37°C. Then 0.25% trypsin/0.02 % ethylenediaminetetraacetic acid (EDTA) was used to digest the confluent cells and to harvest the cells by centrifugation (1000 *g* for 3 min). Afterwards, a hemocytometer was used to calculated cell number of the single cell suspension. After calculation, the cells were resuspended with the medium to incubate with the samples. The HLECs were seeded into the holes of 96-well tissue culture plates (TCPS) containing samples (1.0×10^4 cells per hole) with six parallel replicates, and incubation was conducted for 24 h.

2.5.2. Cell viability

Cell viability of the copolymer brushes was quantitatively evaluated through CCK-8 (Beyotime, China) assay(*5*). After inoculation with the samples for 24 h, the HLECs solution was replaced by 100 μL new medium containing 10 μL CCK-8. After incubation for 2 h at 37°C, water-soluble formazan formed in the solution. The formazan solution (100 μL) was aspirated and added to the well of a new 96-well plate. A microplate reader (Multiskan MK33, Thermo Electron Corporation, China) was used to determine the absorbance at 450 nm. TCPS without any surface modification were used as control.

2.5.3. Cell morphology

Cytoplasmic esterase activity and membrane integrity were indicated through FDA (Sigma) staining. FDA was used to stain the HLECs cultured on the samples for investigation by fluorescence microscopy (Zeiss, Germany) using an excitation wavelength at 488 nm. FDA in acetone (5.0 mg/mL) was prepared as stock solution. Then 5.0 μL stock solutions were diluted with 5.0 mL of phosphate-buffered saline (PBS) to prepare the freshly working solution. Each 96-well plate hole was fed with 20 μL FDA working solution, incubated for 5 min and washed with PBS. The samples were placed on a glass slide for fluorescence microscopy examination. Laser radiation at a wavelength of 488 nm was used to excite the dye. TCPS without any surface modification were used as control.

2.6. Protein adsorption test

Bicinchoninic acid (BCA) protein assay kit (Beyotime Biotechnology, China)(*5*) and bovine serum albumin (BSA) was used to evaluate the anti-adhesive effect of the P(DMAEMA$^+$-*co*-NIPAAm) copolymer brushes against protein adsorption. Firstly, 0.5 mg/mL BSA solution was prepared through diluting the standard solution (5.0 mg/mL) with PBS. The samples were immerged in BSA protein for 2 h and rinsed with 4°C distilled water for 1 min to remove the bound protein. A BCA working solution (0.2 mL) was then added on the samples and incubated at 37°C for 30 min. A microplate reader (Multiskan MK33, Thermo Electron Corporation, China) was used to determine the absorbance at 570 nm. TCPS and PDMS without

any surface modification were used as control.

2.7. *In vitro* antibacterial test

Bacterial live/dead staining and shake-flask culture methods were performed to evaluate the antibacterial property of the copolymer brushes against *E. coli* (ATCC 8739) and *S. aureus* (ATCC 6538) (*43*).

For the shake-flask culture method, the samples were incubated with 10 mL *S. aureus* suspension (1.1×10^5 colony-forming units (CFU)/mL) at 37°C. The bacterial solution was pipetted out at predetermined times and diluted with PBS. The solution (0.2 mL) was spread onto triplicate solid agar and the number of viable bacteria was counted after 24 h incubation. After multiplying by the dilution factor the results were expressed as mean CFU/mL. The bacteria log reduction was calculated using the following formula:

$$\text{Log reduction} = \text{Log (CFU initial bacteria)} - \text{Log (CFU bacteria after incubating)}$$

Bacterial anti-adherence and bactericidal functions of the copolymer brushes were examined using live/dead BacLight bacterial viability kit (L-7012, Invitrogen)(*13*). The copolymer brush coatings and the control PDMS were incubated with *S. aureus* for 24 h and stained in accordance with the instructions. After washing with 37°C or 4°C water, the samples were sealed with tin foil and examined by fluorescence microscopy (Zeiss, Germany).

All data were obtained from at least three independent experiments with six parallel samples and expressed as mean ± standard deviation (SD) of typical images.

3. RESULTS AND DISCUSSION

3.1. Surface-initiated polymerization of the P(DMAEMA$^+$-*co*-NIPAAm) copolymer brush coating

Table 1. Table 2.

The general process for the synthesis of the P(DMAEMA$^+$-*co*-NIPAAm) copolymer brush coating is presented in Figure 1. First, amine groups were generated on the substrate surface through amination using PEI. Second, an initiator layer was generated through covalent binding of the RAFT agent on the substrates by amine coupling through EDC/NHSS. The initiator-modified surfaces were used for polymerization. In the third step, the copolym er brush coating was generated through the surface-initiated RAFT polymerization of NIPAAm and DMAEMA$^+$ monomers. Quaternized DMAEMA$^+$ monomers were prepared by blending DMAEMA and 1-bromoheptane overnight. Each step was verified by XPS, WCA, and spectroscopic ellipsometry measurements. As indicated in Figure 2, when the temperature was 37°C higher than the LCST (~32°C)(*30, 31*), the copolymer coating was in a compressed and hydrophobic state with low moisture content, which could effectively capture and kill bacteria through contact. Positively charged polycations adhered tightly to bacteria with negatively charged surfaces. The quaternized DMAEMA$^+$ component was bactericidal against both gram-negative and gram-positive bacteria(*5, 47*). When the temperature was 4°C lower than the LCST, the copolymer coating swelled by

absorbing water and became capable of releasing dead bacteria. The switching of these functions was achieved based on the transition of the PNIPAAm structure from a bactericidal state to an antifouling state through modulation of the environmental temperature. The functionality of the surface can be simply constructed via surface-initiated RAFT polymerization and can be effectively maintained after several killing–release cycles.

Figure 1. Figure 2.

As shown in Table 1, an aminated surface with a thickness of 3.8 ± 1.6 nm formed on the substrate following PEI pretreatment. A precursor layer of PEI was adsorbed onto all substrates before multilayer assembly(*48*). This kind of substrate treatment is simple and independent of substrate species, so it has already been widely used in coating technology. The most prominent feature of PEI is its high density of amino groups that can be protonated. We have also used 3-aminopropyltriethoxysilane (APTES) to aminate a substrate surface containing hydroxyl groups such as glass or silicon(*46*). However, the thickness of approximately 2 nm was thinner than with the PEI treatment. The surface containing plenty of amino groups was beneficial to surface-initiated polymerization of a dense copolymer brush coating(*49*). After grafting with the RAFT agent, the thickness increased to 6.5 ± 1.7 nm, which indicated that a uniform initiator layer was generated with a thickness of 2.7 nm. A series of P(DMAEMA$^+$-*co*-NIPAAm) copolymers was prepared on the surface and the thickness grew to 16.4–22.4 nm. Compared with the physically adsorbed coating and the self-assembled monolayer, a greater thickness was more likely through RAFT polymerization(*50-52*). As shown in Figure 3 and Table 1, the surface morphology test performed by AFM showed that the copolymer brushes surfaces were very flat and uniform with a low roughness ranging from 4.2 to 4.5 nm ($10\times10\mu m^2$). The AFM images and RMS data also proved the successful of each surfaces modification step. The molecular weight of the obtained copolymer brushes was estimated through adding free RAFT agent into the reactive solution, in which free polymer formed in the solution with similar structure of the polymers on the surface(*53, 54*). The molecular weight of the free polymer could be controlled through changing the polymerization time and feeding ratio of the monomer to the RAFT agent. After polymerization for 24h, the molecular weight and polydispersity index (PDI=M_w/M_n) of copolymer were measured using GPC (Table 1). The M_n of the grafted copolymer brushes ranged from 18, 000 to 21, 000 g/mol with a narrow PDI, which showed that the copolymer brushes of DMAEMA and NIPAAm were synthesized in a controlled manner.

Figure 3. Figure 4.

The elemental composition of the obtained copolymer brushes was determined with high precision by XPS analysis. For the PDMS substrate, there are only C, O, and Si elements, which are also shown after grafting with the RAFT agent (Figure 4a). Because the depth of XPS detection was 1–10 nm(*55*), the results indicated that the thickness of the PEI and RAFT agent coating was less than 10 nm. Four XPS peaks were discernible in the wide scan spectrum with BEs at 532, 397, 284, 102, and 152 eV, which could be attributed to O 1s, N1s, C 1s, Si 2p, and S 2s core level signals, respectively. However, after copolymerization of DMAEMA$^+$ and NIPAAm,

the XPS peaks of S and Si disappeared. A peak for N1s at 400 eV was found, which was ascribed to the tertiary amino groups of the $DMAEMA^+$ on the surface. The measurements proved the successful construction of a P($DMAEMA^+$-*co*-NIPAAm) copolymer brushes with a thickness of more than 10 nm, which was also confirmed by spectroscopic ellipsometry. Moreover, the experimental ratio of C/O/N/S/Si was calculated through XPS integrated area. Compared with a theoretical element calculation, $DMAEMA^+$ monomers were more easily synthesized into the copolymer coating than NIPAAm monomers. As indicated in Table 2, the $DMAEMA^+$/NIPAAm ratio calculated from the experimental copolymer compositions were higher than the feed ratio of $DMAEMA^+$/NIPAAm monomers. The $DMAEMA^+$/NIPAAm ratios in the obtained P($DMAEMA^+$-*co*-NIPAAm) copolymers were 34:66, 57:43 and 76:34 for P3-7, P5-5 and P7-3 respectively. The difference of theoretical/experimental monomer ratio could be due to the reactivity ratio difference of the monomers(*5, 56*). As a result, there was a higher proportion of $DMAEMA^+$ in the obtained copolymer coating than in the feed.

Table 3.

The WCA measurement was conducted to detect the transition from the hydrophilic to the hydrophobic states of the copolymer coating. As shown in Table 3, the WCA values for pristine PDMS and glass were 114.0 ± 3.2° and 42.0 ± 3.1°, respectively, demonstrating the large effect of substrate on surface wettability. PDMS had a much high WCA, reflecting its obvious hydrophobic nature, whereas the glass was hydrophilic with a much lower WCA. More importantly, the NIPAAm-containing coatings showed reduced WCAs as the temperature was lowered from 37°C to 4°C. For the pure PNIPAAm coating (P10-0), there was a 10° (from 62.4 ± 2.3° to 52.9 ± 3.5°) reduction and a 5.5° reduction (from 48.4 ± 2.6° to 42.9 ± 2.8°) for the PDMS and glass substrates, respectively. The changes in WCA for the P3-7, P5-5, P7-3, and P10-0 surfaces also revealed that the greater the proportion of $DMAEMA^+$ in the coating the lower the WCA. However, the pure $PDMAEMA^+$ surface showed no WCA change as a result of decreasing the temperature.

3.2. Cell viability of the material surfaces

It is critical to assess the interaction between the implanted devices and their surrounding environment, especially cell viability, to determine the ultimate functionality of the implants. The biggest advantage of quaternary ammonium salts is their high sterilization efficiency. However, the cytocompatibility of bactericidal surfaces should be examined and determined. To investigate the cytotoxicity of the temperature-triggered bactericidal surfaces, the proliferation and growth of HLECs on the substrates and copolymer brush coatings were determined. As indicated in Figure 5, HLECs activity on the surfaces of TCPS, pristine PDMS, P0-10, and P′3-7 surfaces was high, revealing low cytotoxicity. However, as the proportion of $DMAEMA^+$ increased, the cytotoxicity of the copolymer coating gradually increased. With regards to the P5-5 and P7-3 copolymer brush coatings, the cell viability of the HLECs on the surfaces was lower than 80.0% of that on TCPS, which demonstrated the cytotoxicity of the surface against HLECs. Therefore, in the subsequent antibacterial experiments, the feed ratio of $DMAEMA^+$ and NIPAAm was fixed at 3:7. The ratio of $DMAEMA^+$ to NIPAAm in the obtained copolymer brushes was approximately 34:66, as calculated by XPS integral calculus and equation calculation.

Figure 5.

Figure 6.

As indicated in Figure 6, the FDA images showed the morphology of HLEC adhesion to the surface of P(DMAEMA$^+$-*co*-NIPAAm) copolymer brush coatings with pristine PDMS and TCPS as controls. The HLECs number on the surfaces of pristine PDMS, P0-10, P3-7, and P′3-7 with cell density 12.3×10^3, 10.9×10^3, 11.4×10^3 and 13.4×10^3 cells per mm^2 respectively, was almost the same as that on TCPS (14.5×10^3 cells per mm^2), which confirmed the adequate adhesion and spreading of the cells. However, as the proportion DMAEMA$^+$ in P5-5, P7-3, and P10-0 increased, the number of adhered HLECs gradually decreased (cell density 7.3×10^3, 3.9×10^3 and 3.4×10^3 cells per mm^2, respectively). The cytotoxicity against HLECs could be due to the hydrophobic chains of quaternary ammonium salts that increased HELCs permeability and disrupted the HLECs membranes. This cytotoxicity effect was similar to the bactericidal effects of quaternary ammonium salts against bacteria(*5*). When this observation was considered with the CCK-8 data that the copolymer coating showed obvious cytotoxicity as the increase of DMAEMA$^+$ proportion, we concluded that the copolymer brush coatings had a certain cytotoxic effect on HLECs.

3.3. Bactericidal activity and temperature-triggered release of fouling

The temperature-triggered, switchable bactericidal and fouling release activities of the copolymer brushes were examined through lowering the temperature from 37°C to 4°C against *S. aureus* and *E. coli*. First, the examined samples were incubated with the bacteria to deposit the bacteria and promote their adhesion. In this process, the surfaces of the copolymer brush coatings were in the shrinking hydrophobic state, which promoted the attachment and contact killing of the bacteria. After contact with the bacterial suspension for 24 h, the samples were washed with water at 37°C or 4°C. The bacteria were stained with live/dead two-color fluorescent dye and the fluorescence microscopy (FM) images were obtained to determine the distribution of dead and viable bacteria on the surface. As shown in Figures 7a, 7a′, 8a, and 8a′, there was a large number of living *S. aureus* and *E. coli* on the surface of the glass before washing. However, the number of dead bacteria was few in the absence of the bactericidal component. In comparison, the number of living bacteria on the surface of P3-7 was much lower than on the glass, as indicated in Figures 7d, 7d′, 8d, and 8d′, and there were a large number of red-stained dead bacteria, indicating the efficient bactericidal function of the quaternary ammonium salt component of the copolymer brush coating.

Figure 7.

Figure 8.

To investigate the temperature-responsive activity of the P3-7 surface, the samples were washed with water at different temperatures after attachment of the two species of bacteria. It should be noted that the two species of adhered bacteria did not decrease in number after washing with water at either 37°C or 4°C (Figures 7b, 7b′, 7c, 7c′, 8b, 8b′, 8c, and 8c′). Compared with the control, washing with water at 37°C did not promote the detachment of bacteria from the surface

of P3-7 at all, as shown in Figures 7e, 7e′, 8e, and 8e′. Furthermore, the release capacity of the two species of bacteria was much greater using 4°C water than 37°C water, which proves that fouling was released from the P3-7 copolymer brush coating in a temperature-sensitive manner. The fouling release of the PNIPAAm-based coating arose because the hydrated and swollen state below the LCST led to excellent resistance of P(DMAEMA$^+$-*co*-NIPAAm) to both *S. aureus* and *E. coli*. We predicted that the self-cleaning copolymer brush coating would have bactericidal activity owing to exposure of the PDMAEMA$^+$ functional groups. Although the concentration of *S. aureus* was the same as *E. coli* that was incubated with the samples, the adhered number of the bacteria differed greatly. The number of adhered *S. aureus* on both of PDMS and P3-7 surfaces was much more than *E. coli* on the surfaces before washing. After 4°C water washing, there was almost no *E. coli* remaining on the surface of the P3-7 copolymer brushes coating (Figure 8f and 8f'). However, there was still a few *S. aureus* living or dead remaining on the surface after 4°C water washing as shown in Figure 7f and 7f'. As a result, *S. aureus* adhered more easily to the surface of the implants and was more difficult to remove than *E. coli*.

Figure 9.

To further evaluate the temperature-triggered antifouling property of the copolymer brush coatings, a nonspecific protein adsorption test was carried out with BSA as a model protein. Nonspecific protein adsorption is an important factor that can cause a series of biological reactions including bacterial adhesion and biofilm formation, thrombus formation, immune responses, etc.(*56*). As shown in Figure 9, BSA was readily adsorbed on any kind of surface before washing showing the susceptibility to BSA protein contamination. However, after washing with water at 4°C, there was an obvious difference in the release of fouling BSA from the copolymer brush coatings. The TCPS, PDMS, and P10-0 surfaces showed no BSA adsorption reduction owing to the absence of temperature-triggered antifouling property. With regards to the PNIPAAm-based copolymer brush coatings, most of the proteins were effectively reduced after washing with cold water (4°C). During washing, the PNIPAAm-based copolymers underwent phase transition from a collapsed and hydrophobic state to a hydrophilic swollen state(*36, 57*). The reduction of WCA of the copolymer brush surfaces revealed the transition of surface wettability with the change of ambient temperature. Moreover, the higher the proportion of NIPAAm in the polymer the more BSA was released from the surface.

As shown in Figure 10, the biocidal activity of the P3-7 copolymer brush coating was tested against both *E. coli* and *S. aureus*. Compared with the P0-10, TCPS, and PDMS surfaces, both P10-0 and P3-7 copolymer brush surfaces showed efficient biocidal activity. With regards to the P3-7 copolymers brush, there was a ~2 log *E. coli* reduction and a ~3.5 log *S. aureus* reduction. However, the PDMAEMA$^+$ (P10-0) coating showed stronger bactericidal activity than the P3-7 copolymer brushes with a ~2.8 log *E. coli* reduction and a ~3.9 log *S. aureus* reduction. Notably, the introduction of the PNIPAAm component decreased the bactericidal ability of the coating, which could be a result of the reduction of the bactericidal component contacting with bacteria. Although the PNIPAAm component endowed the surface with a temperature-sensitive hydrophilic–hydrophobic transition nature, the pure PNIPAAm polymer brush coating exhibited no bactericidal activity. More importantly, the P(DMAEMA$^+$-*co*-NIPAAm) surface combined the

bacteria-capturing/contact killing and fouling release composite functions. Taken together, we found that the P3-7 copolymer brush coating performed best and maintained the advantages of both $PDMAEMA^+$ and PNIPAAm. Recent work conducted by Yu *et al.* (*36*) elegantly demonstrated that OPE/PNIPAAm blended films could effectively kill adhered *Staphylococcus epidermidis* (78 ± 5%) and *E. coli* (70 ± 6%) under UVA exposure at 37°C. The bacteria corpse also could be simply eliminated from the surface by washing with 4°C water. The difference in bactericidal efficiency was a result of the structure difference of the bacterial cell wall.

Figure 10.

3.4. Reversibly switchable bactericidal and antifouling activities

We also examined the reversibly switchable bactericidal and antifouling activities of P3-7 copolymer brush coatings through four deposition–release cycles against *S. aureus*, and the results are summarized in Figure 11. After the first deposition of *S. aureus*, the glass was covered with 45.5% living and 7.8% dead bacteria. After washing with cold water, the proportion of living and dead bacteria changed slightly to 43.6% and 7.0%, respectively. In the second cycle, the coverage area of living *S. aureus* greatly increased to 78.4% and the dead *S. aureus* remained at 6.3%. In the third cycle, almost 100% of the surface was covered with *S. aureus*, which indicated the formation of a biofilm. The proportion of dead bacteria slightly decreased to 5.4% of the total area and this could be attributed to the increase of adhered living bacteria number. However, the coverage area of living and dead *S. aureus* on the P3-7 surface was 16.4% and 15.5% respectively for the initial deposition. After cold water washing, the coverage area of living and dead *S. aureus* correspondingly decreased to 1.1% and 1.4%, indicating the antifouling property of the surface. In the second and third cycles, the coverage areas of living and dead *S. aureus* were 12.4%/16.3% and 13.3%/18.5%, respectively. More importantly, the surface exhibited reversibly switchable self-cleaning after cold water washing. The introduction of the $PDMAEMA^+$ component did not interfere with the antifouling property of the copolymer brush surfaces.

Figure 11.

Figure 12.

As discussed earlier, the fouling release activity of the PNIPAAm-based copolymers originated from the phase transition from a collapsed and hydrophobic state to a hydrophilic, swollen state. As shown in Table 2, both the $PDMAEMA^+$ coating and the glass substrate surfaces were quite hydrophilic (about 42°), which was conducive to the release of adhered bacteria. Furthermore, the reversibly switchable bactericidal function of the P3-7 copolymer brush coating after cold water washing was also explored against both *S. aureus* and *E. coli*. As expected, the surface exhibited strong and reversibly switchable bactericidal activity. In light of the generally accepted mechanism for the bactericidal property of polycations, the positively charged $PDMAEMA^+$ component interacted electrostatically with phospholipids and proteins with negative charges on bacterial surfaces. The interaction may have impaired the bacterial cytoplasmic membrane permeability, which led to the cytoplasmic constituent losses and the bacteria death. In this system,

the positively charged copolymer brush surfaces could effectively attract and capture bacteria through electrostatic interactions. In comparison, the bactericidal efficiency against *S. aureus* (~3 log reduction) was stronger than against *E. coli* (~2 log reduction), as indicated in Figure 12. This finding was consistent with previous studies that demonstrated that quaternary ammonium salts provide stronger bactericidal property against *S. aureus* (gram-positive) than against *E. coli* (gram-negative). The reason for this could be the difference in the cell wall structures of these two kinds of bacteria(*58, 59*). In comparison with gram-positive bacteria, gram-negative bacteria have more lipopolysaccharides (LPSs) in the cell wall membrane, which create a secondary LPS barrier to further protect the bacteria against lysis by quaternary ammonium salts.

4. CONCLUSIONS

In summary, we developed a temperature-triggered, reversibly switchable bactericidal and antifouling surface with the dual capability of capture-killing and fouling release. We demonstrated that it was effective and controllable to use surface-initiated RAFT polymerization to combine thermally responsive NIPAAm and bactericidal quaternary ammonium salt $DMAEMA^+$ components. As the temperature was higher than the LCST, the copolymer brush coating was able to capture and effectively kill bacteria by virtue of the quaternary ammonium $DMAEMA^+$ component, which served as a biocide. What's more, after the killing process, the adhered bacteria corpse on the P($DMAEMA^+$-*co*-NIPAAm) surface could be readily released by lowering the temperature. The copolymer demonstrated reversibly switchable bactericidal and antifouling activity through four deposition–release cycles and had excellent temperature-triggered self-cleaning capability. Moreover, the bactericidal efficiency of the coating was restored after cold water washing, and the copolymer demonstrated a ~3 log reduction in gram-positive *S. aureus* and a ~2 log reduction in gram-negative *E. coli* after incubation for four deposition–fouling release cycles. To the best of our knowledge, despite many modification strategies to resist fouling, no anti-adhesive surface that is capable of resisting bacteria and protein adhesion in the long-term has been developed. The temperature-responsive PNIPAAm incorporated in our system can repeatedly kill bacteria and resist fouling in response to a change in the ambient water temperature.

5. ACKNOWLEDGEMENTS

We greatly appreciate help from the National Natural Science Foundation of China (51403158, 81271703, 31570959), the Natural Science Foundation of Zhejiang Province (LY12H12005, LQ14C100002), and the Wenzhou Bureau of Science and Technology (2013S0458).

REFERENCES

(1) Wang, B. L., Jin, T. W., Xu, Q. W., Liu, H. H., Ye, Z., and Chen, H. (2016) Direct Loading and Tunable Release of Antibiotics from Polyelectrolyte Multilayers To Reduce Bacterial Adhesion and Biofilm Formation. *Bioconjugate Chem 27*, 1305-1313.

(2) Shivapooja, P., Yu, Q., Orihuela, B., Mays, R., Rittschof, D., Genzer, J., and Lopez, G. P. (2015) Modification of Silicone Elastomer Surfaces with Zwitterionic Polymers: Short-Term Fouling Resistance and Triggered Biofouling Release. *Acs Applied Materials & Interfaces 7*, 25586-25591.

(3) Wei, T., Yu, Q., Zhan, W., and Chen, H. (2016) A Smart Antibacterial Surface for the On-Demand Killing and Releasing of Bacteria. *Advanced Healthcare Materials 5*, 449-456.

(4) Wang, B. L., Han, Y. M., Lin, Q. K., Liu, H. H., Shen, C. H., Nan, K. H., and Chen, H. (2016) In vitro and in vivo evaluation of xanthan gum-succinic anhydride hydrogels for the ionic strength-sensitive release of antibacterial agents. *Journal of Materials Chemistry B 4*, 1853-1861.

(5) Wang, B. L., Jin, T. W., Han, Y. M., Shen, C. H., Li, Q., Lin, Q. K., and Chen, H. (2015) Bio-inspired terpolymers containing dopamine, cations and MPC: a versatile platform to construct a recycle antibacterial and antifouling surface. *Journal of Materials Chemistry B 3*, 5501-5510.

(6) Humblot, V., Yala, J. F., Thebault, P., Boukerma, K., Hequet, A., Berjeaud, J. M., and Pradier, C. M. (2009) The antibacterial activity of Magainin I immobilized onto mixed thiols Self-Assembled Monolayers. *Biomaterials 30*, 3503-3512.

(7) Wang, B.-l., Wang, J.-l., Li, D.-d., Ren, K.-f., and Ji, J. (2012) Chitosan/poly (vinyl pyrollidone) coatings improve the antibacterial properties of poly(ethylene terephthalate). *Applied Surface Science 258*, 7801-7808.

(8) Faure, E., Falentin-Daudre, C., Lanero, T. S., Vreuls, C., Zocchi, G., Van De Weerdt, C., Martial, J., Jerome, C., Duwez, A. S., and Detrembleur, C. (2012) Functional Nanogels as Platforms for Imparting Antibacterial, Antibiofilm, and Antiadhesion Activities to Stainless Steel. *Advanced Functional Materials 22*, 5271-5282.

(9) Vepari, C., Matheson, D., Drummy, L., Naik, R., and Kaplan, D. L. (2010) Surface modification of silk fibroin with poly(ethylene glycol) for antiadhesion and antithrombotic applications. *Journal of Biomedical Materials Research Part A 93A*, 595-606.

(10) Lai, Y. K., Lin, L. X., Pan, F., Huang, J. Y., Song, R., Huang, Y. X., Lin, C. J., Fuchs, H., and Chi, L. F. (2013) Bioinspired Patterning with Extreme Wettability Contrast on TiO2 Nanotube Array Surface: A Versatile Platform for Biomedical Applications. *Small 9*, 2945-2953.

(11) Wang, B. L., Liu, X. S., Ji, Y., Ren, K. F., and Ji, J. (2012) Fast and long-acting antibacterial properties of chitosan-Ag/polyvinylpyrrolidone nanocomposite films. *Carbohydrate Polymers 90*, 8-15.

(12) Yu, Q., Wu, Z. Q., and Chen, H. (2015) Dual-function antibacterial surfaces for biomedical applications. *Acta Biomaterialia 16*, 1-13.

(13) Wang, B.-l., Ren, K.-f., Wang, H. C. J.-l., and Ji, J. (2013) Construction of Degradable Multilayer Films for Enhanced Antibacterial Properties. *Acs Applied Materials & Interfaces 5*, 4136-4143.

(14) Ista, L. K., Dascier, D., Ji, E., Parthasarathy, A., Corbitt, T. S., Schanze, K. S., and WhittenIi, D. G. (2011) Conjugated-Polyelectrolyte-Grafted Cotton Fibers Act as "Micro Flypaper" for

the Removal and Destruction of Bacteria. *Acs Applied Materials & Interfaces 3*, 2932-2937.

(15) Wang, B. L., Lin, Q. K., Jin, T. W., Shen, C. H., Tang, J. M., Hana, Y. M., and Chen, H. (2015) Surface modification of intraocular lenses with hyaluronic acid and lysozyme for the prevention of endophthalmitis and posterior capsule opacification. *Rsc Advances 5*, 3597-3604.

(16) Zhu, X., and Loh, X. J. (2015) Layer-by-layer assemblies for antibacterial applications. *Biomaterials Science 3*, 1505-1518.

(17) Wang, B. L., Liu, H. H., Zhang, B. J., Han, Y. M., Shen, C. H., Lin, Q. K., and Chen, H. (2016) Development of antibacterial and high light transmittance bulk materials: Incorporation and sustained release of hydrophobic or hydrophilic antibiotics. *Colloids and Surfaces B-Biointerfaces 141*, 483-490.

(18) Huang, C.-J., Chen, Y.-S., and Chang, Y. (2015) Counterion-Activated Nanoactuator: Reversibly Switchable Killing/Releasing Bacteria on Polycation Brushes. *Acs Applied Materials & Interfaces 7*, 2415-2423.

(19) Ting Wei, Q. Y., Wenjun Zhan and Hong Chen. (2016) Antibacterial Surfaces: A Smart Antibacterial Surface for the On-Demand Killing and Releasing of Bacteria. *Advanced Healthcare Materials 5*, 449-456.

(20) Lu, Y., Yue, Z. G., Wang, W., and Cao, Z. Q. (2015) Strategies on designing multifunctional surfaces to prevent biofilm formation. *Frontiers of Chemical Science and Engineering 9*, 324-335.

(21) Cao, Z. Q., Mi, L., Mendiola, J., Ella-Menye, J. R., Zhang, L., Xue, H., and Jiang, S. Y. (2012) Reversibly Switching the Function of a Surface between Attacking and Defending against Bacteria. *Angew Chem Int Edit 51*, 2602-2605.

(22) Cheng, G., Zhang, Z., Chen, S. F., Bryers, J. D., and Jiang, S. Y. (2007) Inhibition of bacterial adhesion and biofilm formation on zwitterionic surfaces. *Biomaterials 28*, 4192-4199.

(23) Mi, L., and Jiang, S. Y. (2014) Integrated Antimicrobial and Nonfouling Zwitterionic Polymers. *Angew Chem Int Edit 53*, 1746-1754.

(24) Mi, L., Xue, H., Li, Y. T., and Jiang, S. Y. (2011) A Thermoresponsive Antimicrobial Wound Dressing Hydrogel Based on a Cationic Betaine Ester. *Advanced Functional Materials 21*, 4028-4034.

(25) Yu, Q., Ista, L. K., and Lopez, G. P. (2014) Nanopatterned antimicrobial enzymatic surfaces combining biocidal and fouling release properties. *Nanoscale 6*, 4750-4757.

(26) Yu, Q., Cho, J., Shivapooja, P., Ista, L. K., and Lopez, G. P. (2013) Nanopatterned Smart Polymer Surfaces for Controlled Attachment, Killing, and Release of Bacteria. *Acs Applied Materials & Interfaces 5*, 9295-9304.

(27) Radhakumary, C., Antonty, M., and Sreenivasan, K. (2011) Drug loaded thermoresponsive and cytocompatible chitosan based hydrogel as a potential wound dressing. *Carbohydrate Polymers 83*, 705-713.

(28) Laloyaux, X., Fautre, E., Blin, T., Purohit, V., Leprince, J., Jouenne, T., Jonas, A. M., and Glinel, K. (2010) Temperature-Responsive Polymer Brushes Switching from Bactericidal to Cell-Repellent. *Advanced Materials 22*, 5024-+.

(29) Chang, Y., Yandi, W., Chen, W.-Y., Shih, Y.-J., Yang, C.-C., Chang, Y., Ling, Q.-D., and Higuchi, A. (2010) Tunable Bioadhesive Copolymer Hydrogels of Thermoresponsive Poly(N-isopropyl acrylamide) Containing Zwitterionic Polysulfobetaine. *Biomacromolecules*

11, 1101-1110.

(30) Pappas, H. C., Phan, S., Yoon, S., Edens, L. E., Meng, X. L., Schanze, K. S., Whitten, D. G., and Keller, D. J. (2015) Self-Sterilizing, Self-Cleaning Mixed Polymeric Multifunctional Antimicrobial Surfaces. *Acs Applied Materials & Interfaces 7*, 27632-27638.

(31) Chen, X., Bi, S. Y., Shi, C. C., He, Y., Zhao, L. Z., and Chen, L. (2013) Temperature-sensitive membranes prepared from blends of poly(vinylidene fluoride) and poly(N-isopropylacrylamides) microgels. *Colloid and Polymer Science 291*, 2419-2428.

(32) Schwartz, V. B., Thetiot, F., Ritz, S., Puetz, S., Choritz, L., Lappas, A., Foerch, R., Landfester, K., and Jonas, U. (2012) Antibacterial Surface Coatings from Zinc Oxide Nanoparticles Embedded in Poly(N-isopropylacrylamide) Hydrogel Surface Layers. *Advanced Functional Materials 22*, 2376-2386.

(33) Lin, S. Y., Chen, K. S., and Liang, R. C. (2001) Design and evaluation of drug-loaded wound dressing having thermo responsive, adhesive, absorptive and easy peeling properties. *Biomaterials 22*, 2999-3004.

(34) Berndt, E., Behnke, S., Dannehl, A., Gajda, A., Wingender, J., and Ulbricht, M. (2010) Functional coatings for anti-biofouling applications by surface segregation of block copolymer additives. *Polymer 51*, 5910-5920.

(35) Kurkuri, M. D., Nussio, M. R., Deslandes, A., and Voelcker, N. H. (2008) Thermosensitive copolymer coatings with enhanced wettability switching. *Langmuir 24*, 4238-4244.

(36) Yu, Q., Ge, W. Y., Atewologun, A., Stiff-Roberts, A. D., and Lopez, G. P. (2015) Antimicrobial and bacteria-releasing multifunctional surfaces: Oligo (p-phenylene-ethynylene)/poly (N-isopropylacrylamide) films deposited by RIR-MAPLE. *Colloids and Surfaces B-Biointerfaces 126*, 328-334.

(37) Fu, J. H., Ji, J., Yuan, W. Y., and Shen, J. C. (2005) Construction of anti-adhesive and antibacterial multilayer films via layer-by-layer assembly of heparin and chitosan. *Biomaterials 26*, 6684-6692.

(38) Dong, H., Huang, J., Koepsel, R. R., Ye, P., Russell, A. J., and Matyjaszewski, K. (2011) Recyclable Antibacterial Magnetic Nanoparticles Grafted with Quaternized Poly(2-(dimethylamino)ethyl methacrylate) Brushes. *Biomacromolecules 12*, 1305-1311.

(39) Zammarelli, N., Luksin, M., Raschke, H., Hergenroder, R., and Weberskirch, R. (2013) "Grafting-from" Polymerization of PMMA from Stainless Steel Surfaces by a RAFT-Mediated Polymerization Process. *Langmuir 29*, 12834-12843.

(40) Fadida, T., Kroupitski, Y., Peiper, U. M., Bendikov, T., Sela, S., and Poverenov, E. (2014) Air-ozonolysis to generate contact active antimicrobial surfaces: Activation of polyethylene and polystyrene followed by covalent graft of quaternary ammonium salts. *Colloids and Surfaces B-Biointerfaces 122*, 294-300.

(41) Wang, J. L., Zhu, H., Chen, G. J., Hu, Z. J., Weng, Y. Y., Wang, X. B., and Zhang, W. D. (2014) Controlled Synthesis and Self-Assembly of Dopamine-Containing Copolymer for Honeycomb-Like Porous Hybrid Particles. *Macromolecular Rapid Communications 35*, 1061-1067.

(42) Cado, G., Aslam, R., Seon, L., Garnier, T., Fabre, R., Parat, A., Chassepot, A., Voegel, J. C., Senger, B., Schneider, F., Frere, Y., Jierry, L., Schaaf, P., Kerdjoudj, H., Metz-Boutigue, M. H., and Boulmedais, F. (2013) Self-Defensive Biomaterial Coating Against Bacteria and Yeasts: Polysaccharide Multilayer Film with Embedded Antimicrobial Peptide. *Advanced Functional*

Materials 23, 4801-4809.

(43) Wang, B. L., Ye, Z., Tang, Y. H., Liu, H. H., Lin, Q. K., Chen, H., and Nan, K. H. (2016) Loading of Antibiotics into Polyelectrolyte Multilayers after Self-Assembly and Tunable Release by Catechol Reaction. *Journal of Physical Chemistry C 120*, 6145-6155.

(44) Roy, D., Knapp, J. S., Guthrie, J. T., and Perrier, S. (2008) Antibacterial cellulose fiber via RAFT surface graft polymerization. *Biomacromolecules 9*, 91-99.

(45) Westman, E. H., Ek, M., Enarsson, L. E., and Wagberg, L. (2009) Assessment of Antibacterial Properties of Polyvinylamine (PVAm) with Different Charge Densities and Hydrophobic Modifications. *Biomacromolecules 10*, 1478-1483.

(46) Wang, B., Jin, T., Han, Y., Shen, C., Li, Q., Tang, J., Chen, H., and Lin, Q. (2016) Surface-initiated RAFT polymerization of p (MA POSS-co-DMAEMA(+)) brushes on PDMS for improving antiadhesive and antibacterial properties. *International Journal of Polymeric Materials and Polymeric Biomaterials 65*, 55-64.

(47) Cuthbert, T. J., Guterman, R., Ragogna, P. J., and Gillies, E. R. (2015) Contact active antibacterial phosphonium coatings cured with UV light. *Journal of Materials Chemistry B 3*, 1474-1478.

(48) Li, Q., Quinn, J. F., and Caruso, F. (2005) Nanoporous polymer thin films via polyelectrolyte templating. *Advanced Materials 17*, 2058-2062.

(49) Lin, Q. K., Xu, X., Wang, B. L., Shen, C. H., Tang, J. M., Han, Y. M., and Chen, H. (2015) Hydrated polysaccharide multilayer as an intraocular lens surface coating for biocompatibility improvements. *Journal of Materials Chemistry B 3*, 3695-3703.

(50) Li, X., Cao, Y., Kang, G., Yu, H., and Liu, Z. (2014) Preparation of Antimicrobial Nanofiltration Membrane via Self-polymerization of Dopamine and Surface Grafting of PHGH. *Chemical Journal of Chinese Universities-Chinese 35*, 2026-2030.

(51) Le, X. T., Doan, N. D., Dequivre, T., Viel, P., and Palacin, S. (2014) Covalent Grafting of Chitosan onto Stainless Steel through Aryldiazonium Self-Adhesive Layers. *Acs Applied Materials & Interfaces 6*, 9085-9092.

(52) Bolduc, O. R., Correia-Ledo, D., and Masson, J. F. (2012) Electroformation of Peptide Self-Assembled Monolayers on Gold. *Langmuir 28*, 22-26.

(53) Huang, J. Y., Murata, H., Koepsel, R. R., Russell, A. J., and Matyjaszewski, K. (2007) Antibacterial polypropylene via surface-initiated atom transfer radical polymerization. *Biomacromolecules 8*, 1396-1399.

(54) Marc Husseman , E. E. M., † Molly McNamara ,† Mathew Mate ,† David Mecerreyes ,† Didier G. Benoit ,† James L. Hedrick ,*† Paul Mansky ,‡ E. Huang ,‡ Thomas P. Russell ,*‡ and Craig J. Hawker. (1999) Controlled Synthesis of Polymer Brushes by “Living” Free Radical Polymerization Techniques. *Macromolecules 32*, 1424–1431.

(55) Ozcam, A. E., Roskov, K. E., Spontak, R. J., and Genzer, J. (2012) Generation of functional PET microfibers through surface-initiated polymerization. *Journal of Materials Chemistry 22*, 5855-5864.

(56) Long, L. X., Yuan, X. B., Li, Z. Y., Li, K., Cui, Z. D., Zhang, X. J., and Sheng, J. (2014) Anti-fouling properties of polylactic acid film modified by pegylated phosphorylcholine derivatives. *Materials Chemistry and Physics 143*, 929-938.

(57) Zhou, S. Y., Xue, A. L., Zhang, Y., Li, M. S., Wang, J. G., Zhao, Y. J., and Xing, W. H. (2014) Fabrication of temperature-responsive ZrO2 tubular membranes, grafted with poly

(N-isopropylacrylamide) brush chains, for protein removal and easy cleaning. *Journal of Membrane Science 450*, 351-361.

(58) Xing, K., Chen, X. G., Kong, M., Liu, C. S., Cha, D. S., and Park, H. J. (2009) Effect of oleoyl-chitosan nanoparticles as a novel antibacterial dispersion system on viability, membrane permeability and cell morphology of Escherichia coli and Staphylococcus aureus. *Carbohydrate Polymers 76*, 17-22.

(59) Gibney, K. A., Sovadinova, I., Lopez, A. I., Urban, M., Ridgway, Z., Caputo, G. A., and Kuroda, K. (2012) Poly(ethylene imine)s as Antimicrobial Agents with Selective Activity. *Macromolecular Bioscience 12*, 1279-1289.

Table 1. Summary of the various characteristics of the P(DMAEMA$^+$-*co*-NIPAAm) copolymer brush coating.

Table 2. Component analysis of the copolymer brush coating calculated through X-ray photoelectron spectroscopy (XPS) spectra.

Table 3. Changes in the water contact angle at different temperatures on polydimethylsiloxane (PDMS) and glass.

Figure 1. Schematic illustration of the synthesis process of P(DMAEMA$^+$-*co*-NIPAAm) copolymer brush coating.

Figure 2. Schematic illustration of temperature-responsive copolymer brush surfaces with reversibly switchable bactericidal and antifouling activities.

Figure 3. Atomic Force Microscopy (AFM) images of surfaces of (a) PDMS, (b) PEI, (c) RAFT agent and (d) P3-7 copolymer brush coating.

Figure 4. Wide-scan X-ray photoelectron spectroscopy (XPS) spectra collected from polydimethylsiloxane (PDMS) surface: (a) after reversible addition-fragmentation chain transfer (RAFT) agent grafting; (b) after surface-initiated polymerization of P3-7.

Figure 5. Cell viability assay of human lens epithelial cells (HLECs) cultured on the surfaces of tissue culture plates (TCPS), pristine polydimethylsiloxane (PDMS), and P0-10-, P3-7-, P5-5-, P7-3-, P10-0-, and P′3-7-modified PDMS for 24 h. The absorbance of the diluted cell counting kit solution has been deducted from each data point and the statistical significance is indicated by different letters ($p < 0.05$).

Figure 6. Growth and morphology of human lens epithelial cells (HLECs) stained with fluorescein diacetate (FDA) after 24 h of incubation on the surfaces of tissue culture plates (a) TCPS, (b) pristine polydimethylsiloxane (PDMS), and (c) P0-10-, (d) P3-7-, (e) P5-5-, (f) P7-3-, (g) P10-0-, and (h) P′3-7-modified PDMS, under fluorescence microscopy (magnification 20×).

Figure 7. Fluorescent microscopy images of live/dead staining of *Staphylococcus aureus* on pristine glass and P3-7 copolymer brush coating-modified glass before washing (a, a′), (d, d′), after 37°C water washing (b, b′), (e, e′) or after 4°C water washing (c, c′), (f, f′) at 24 h. Green indicates live bacteria and red indicates dead bacteria under fluorescence microscopy (magnification 10×).

Figure 8. Fluorescent microscopy images of live/dead staining of *Escherichia coli* on pristine glass and P3-7 copolymer brush coating-modified glass before washing (a, a′), (d, d′), after 37°C water washing (b, b′), (e, e′) or after 4°C water washing (c, c′), (f, f′) at 24 h. Green indicates live bacteria and red indicates dead bacteria under fluorescence microscopy (magnification 10×).

Figure 9. Bovine serum albumin (BSA) adsorption onto tissue culture plates (TCPS), pristine polydimethylsiloxane (PDMS), and P0-10-, P3-7-, P5-5-, P7-3-, and P10-0-modified PDMS. The statistical significance is indicated by different letters ($p < 0.05$).

Figure 10. Killing efficiency of P0-10, P3-7, and P10-0 copolymer brush coating-modified polydimethylsiloxane (PDMS) against *Escherichia coli* and *Staphylococcus aureus* with tissue culture plates (TCPS) and pristine PDMS as controls.

Figure 11. Reversibly switchable bactericidal activity of P3-7 copolymer brush coating-modified glass against *Escherichia coli* and *Staphylococcus aureus* after four deposition–release cycles.

Figure 12. Reversibly switchable fouling release activity of pristine glass and P3-7 copolymer brush coating-modified glass against *Staphylococcus aureus* after four deposition–release cycles.

Table 1

Test method	PDMS	PEI	RAFT	P0-10	P3-7	P5-5	P7-3	P10-0
Thickness*/nm	N/A	3.8±1.6	6.5±1.7	16.4±3.2	18.4±2.8	18.4±2.7	20.4±3.2	22.4±2.3
RMS/nm	2.8±0.3	2.4±0.5	3.4±0.4	4.2±0.4	3.9±0.3	4.5±0.5	4.3±0.6	2.9±0.5
$M_n/M_w(\times 10^3)$	-	-	-	18.1/27.5	21.4/31.7	17.8/26.2	19.4/29.1	18.6/27.2
PDI	-	-	-	1.52	1.48	1.47	1.50	1.46

*Thickness measurement was did on silicon wafer

Table 2

Percent/%	PDMS	PEI	RAFT	P0-10	P3-7	P5-5	P7-3	P10-0
C (T/E*)	50.0/51.0	66.7/63.2	72.2/70.8	75.0/75.4	74.3/74.6	73.9/74.1	73.4/73.5	72.7/72.8
O (T/E)	25.0/24.4	0/18.4	11.1/11.3	12.5/12.3	14.2/13.9	15.4/14.9	16.5/16.3	18.2/18.0
N (T/E)	-/-	33.3/13.6	5.6/8.4	12.5/12.3	11.5/11.5	10.8/11.0	10.1/10.2	9.1/9.2
S (T/E)	-/-	-/-	11.1/4.5	-/-	-/-	-/-	-/-	-/-
Si (T/E)	25.0/24.6	0/5.8	0/5.0	-/-	-/-	-/-	-/-	-/-
$DMAEMA^+$/NIPAAm (E)	-/-	-/-	-/-	0/100	34/66	57/43	76/24	100/0

* E/T: Experimental/theoretical

Table 3

Static contact angle/º	Substrate	P0-10	P3-7	P5-5	P7-3	P10-0
On PDMS/37°C	114.0 ± 3.2	75.1±1.6	71.4±2.8	66.4±2.7	63.4±3.2	62.4±2.3
On PDMS/4°C	114.3 ± 3.8	65.6±2.3	65.9±2.4	60.5±3.2	54.3±0.6	62.9±3.5
On glass/37°C	42.0 ± 3.1	65.1±2.3	61.4±3.1	56.4±2.3	53.4±2.5	48.4±2.6
On glass/4°C	42.3 ± 2.8	54.6±2.0	55.9±2.6	50.5±2.2	48.3±2.1	48.9±2.8

Figure 1

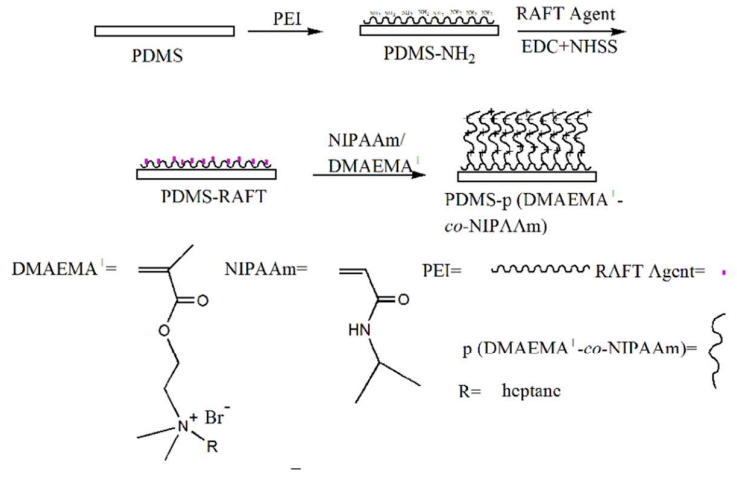

Figure 2

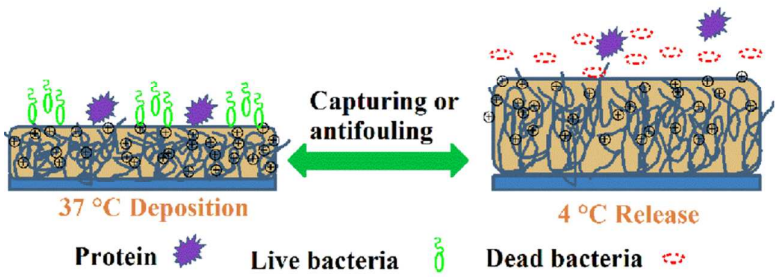

Figure 3

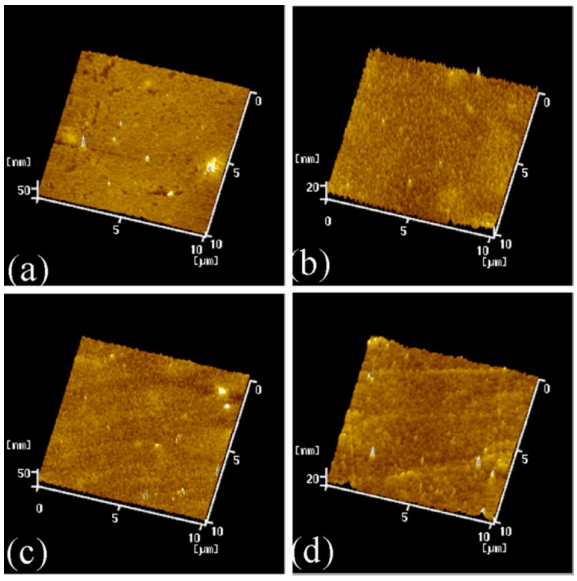

Figure 4

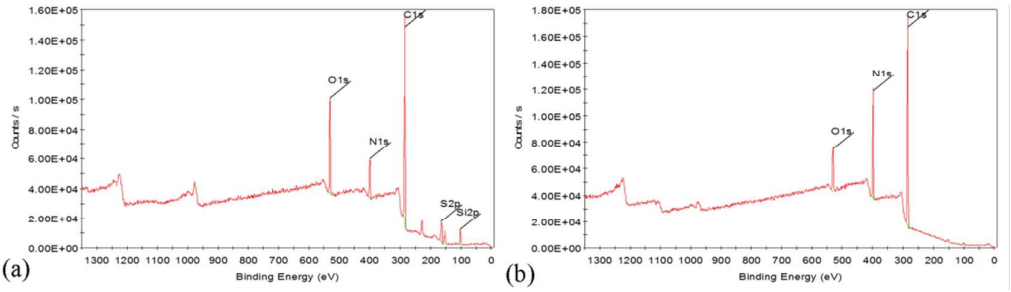

Figure 5

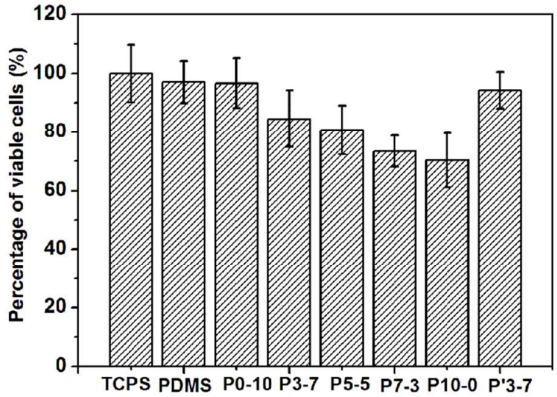

Figure 6

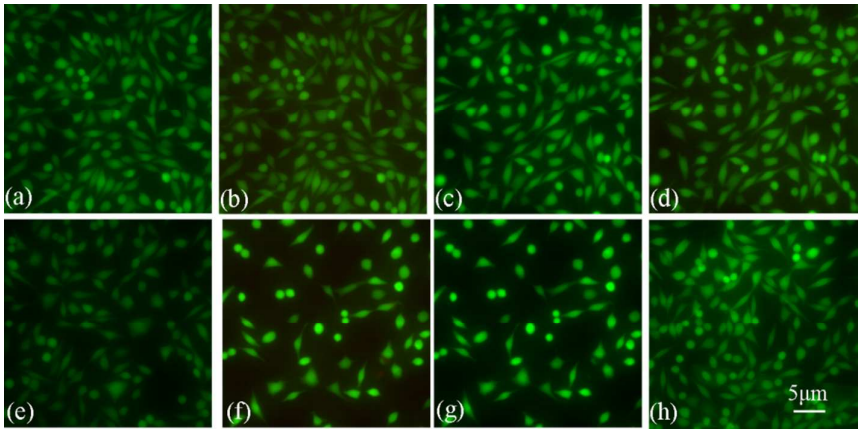

Figure 7

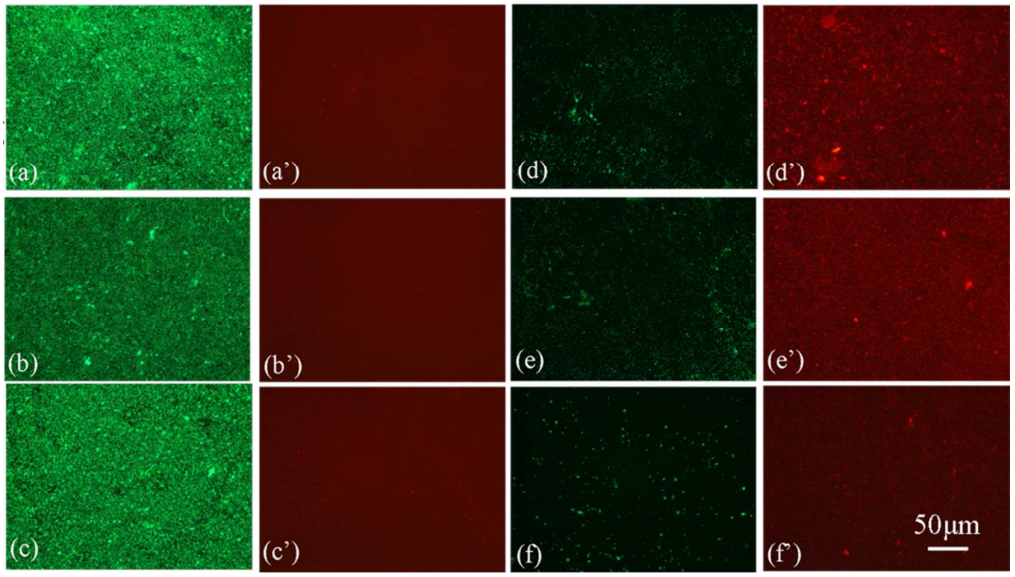

Figure 8

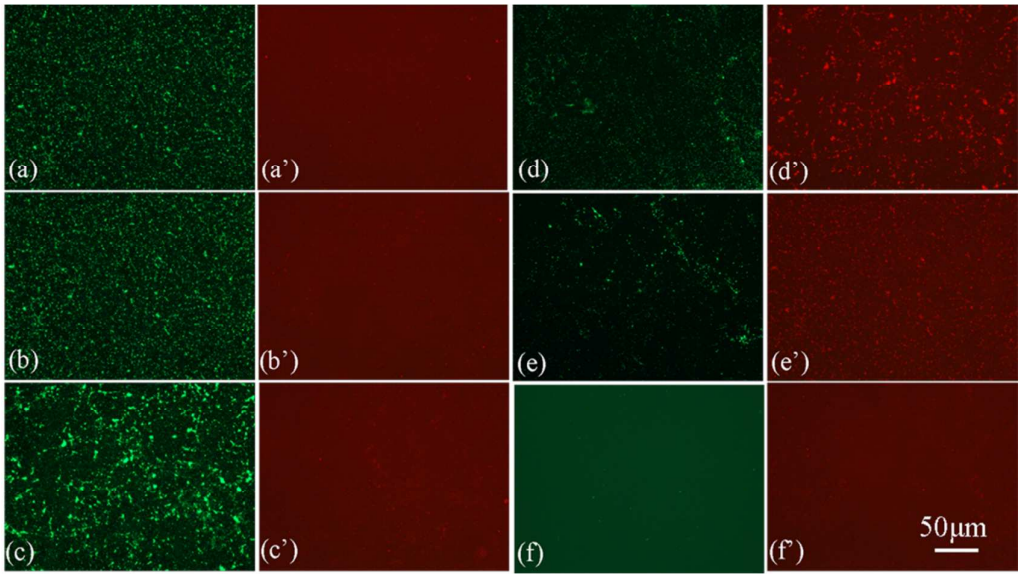

Figure 9

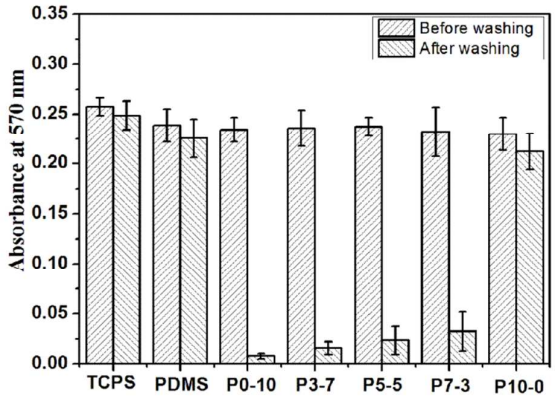

Figure 10

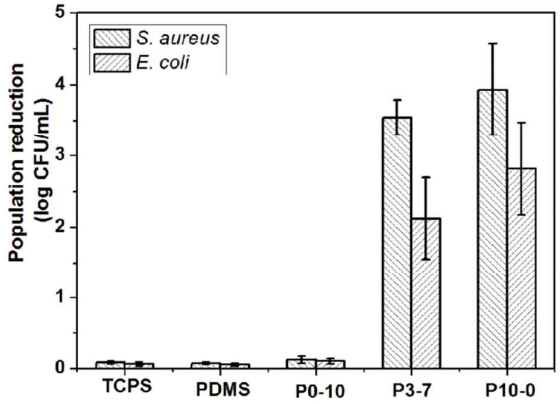

Figure 11

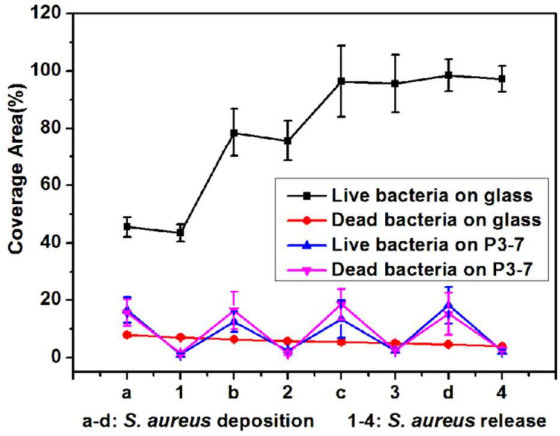

Figure 12

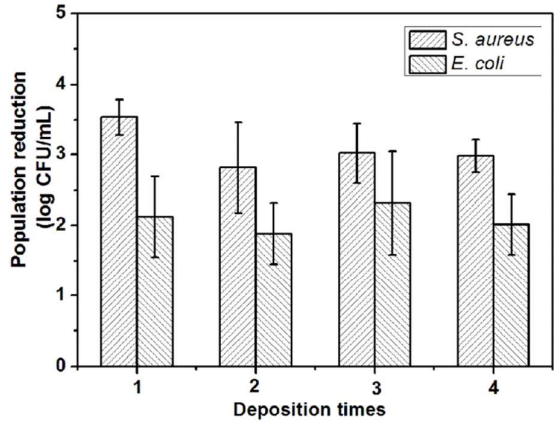

TOC image

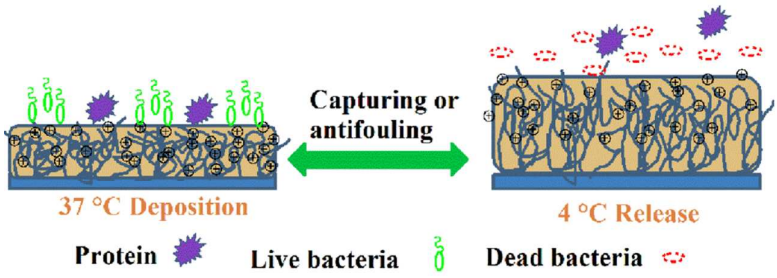
Capturing or
antifouling
37 °C Deposition
4 °C Release
Protein
Live bacteria
Dead bacteria